Darcy–Forchheimer Flow With Viscous Dissipation in a Horizontal Porous Layer: Onset of Convective Instabilities

A. Barletta
e-mail: antonio.barletta@mail.ing.unibo.it

M. Celli
e-mail: michele.celli@mail.ing.unibo.it

Dipartimento di Ingegneria Energetica, Nucleare e del Controllo Ambientale (DIENCA), Università di Bologna, Via dei Colli 16, I-40136 Bologna, Italy

D. A. S. Rees
Department of Mechanical Engineering, University of Bath, Bath BA2 7AY, UK
e-mail: d.a.s.rees@bath.ac.uk

Parallel Darcy–Forchheimer flow in a horizontal porous layer with an isothermal top boundary and a bottom boundary, which is subject to a third kind boundary condition, is discussed by taking into account the effect of viscous dissipation. This effect causes a nonlinear temperature profile within the layer. The linear stability of this nonisothermal base flow is then investigated with respect to the onset of convective rolls. The third kind boundary condition on the bottom boundary plane may imply adiabatic/isothermal conditions on this plane when the Biot number is either zero (adiabatic) or infinite (isothermal). The solution of the linear equations for the perturbation waves is determined by using a fourth order Runge–Kutta scheme in conjunction with a shooting technique. The neutral stability curve and the critical value of the governing parameter $R=GePe^2$ are obtained, where Ge is the Gebhart number and Pe is the Péclet number. Different values of the orientation angle between the direction of the basic flow and the propagation axis of the disturbances are also considered. [DOI: 10.1115/1.3090815]

Keywords: laminar flow, mixed convection, Darcy–Forchheimer model, porous medium, linear stability, viscous dissipation

1 Introduction

Convective instabilities in porous layers have been the subject of very many investigations in the past decades. A cornerstone in this field is the so-called Horton–Rogers–Lapwood (HRL) problem [1,2]. This problem consists of the linear stability analysis of a fluid at rest in a porous plane layer where the bottom isothermal boundary is held at a relatively high temperature while the top isothermal boundary is at a lower temperature. Physically, the HRL problem is the porous medium analog of the classical Bénard problem for a clear fluid and is often called the Darcy–Bénard problem. The HRL problem admits a very simple analytical solution for the basic state, which is compatible with both the Darcy and the Darcy–Forchheimer models. Several other variants of the original HRL problem have been investigated in the past years. Reviews of the wide literature on this subject may be found in Refs. [3–5]. An important problem closely related to the HRL problem is the much less well-known Prats problem [6]. This latter problem is the linear stability analysis, according to the Darcy model, of the HRL configuration in the presence of a uniform horizontal flow.

The present paper investigates the onset of linear instabilities in a horizontal porous layer induced by the viscous heating effect, a topic on which very few papers have been published (see Refs. [7–9]). Unlike in the Prats problem [6], the vertical temperature gradient causing the onset of convective rolls is not imposed externally through the boundary conditions. Rather, it is the internally generated heat due to viscous friction that causes the vertical temperature gradient and thus gives rise to the possibility of convective instability. In this paper, the top boundary surface is considered to be isothermal, while the bottom boundary is subject to a thermal boundary condition of the third kind for which a Biot number, Bi, may be defined. This latter boundary condition is studied including the two limiting cases, $\mathrm{Bi}\to 0$ (adiabatic boundary) and $\mathrm{Bi}\to\infty$ (isothermal boundary). A linear stability analysis of oblique rolls, which are inclined arbitrarily with respect to the uniform base flow direction, is performed. The disturbance equations are solved numerically by a fourth order Runge–Kutta method. The governing parameter for the onset of convective instabilities is defined as $R=\mathrm{GePe}^2$, where Ge is the Gebhart number and Pe is the Péclet number.

2 Mathematical Model

A laminar buoyant flow in a horizontal parallel channel with height L is considered (see Fig. 1). Both the Darcy–Forchheimer model and the Boussinesq approximation are invoked. The horizontal boundary walls, $\bar{y}=0,L$, exchange heat with an external environment at temperature T_w: the top surface is taken to be perfectly isothermal at temperature T_w (infinite Biot number), while the bottom surface is taken to be imperfectly isothermal (finite Biot number).

The governing mass, momentum, and energy balance equations may be expressed as

$$\bar{\nabla}\cdot\bar{\mathbf{u}}=0 \tag{1}$$

$$\frac{\nu}{K}\left(1+\frac{C_f\sqrt{K}}{\nu}\sqrt{\bar{\mathbf{u}}\cdot\bar{\mathbf{u}}}\right)\bar{u}=-\frac{1}{\rho}\frac{\partial\bar{P}}{\partial\bar{x}} \tag{2}$$

$$\frac{\nu}{K}\left(1+\frac{C_f\sqrt{K}}{\nu}\sqrt{\bar{\mathbf{u}}\cdot\bar{\mathbf{u}}}\right)\bar{v}=-\frac{1}{\rho}\frac{\partial\bar{P}}{\partial\bar{y}}+\beta g(\bar{T}-\bar{T}_w) \tag{3}$$

$$\frac{\nu}{K}\left(1+\frac{C_f\sqrt{K}}{\nu}\sqrt{\bar{\mathbf{u}}\cdot\bar{\mathbf{u}}}\right)\bar{w}=-\frac{1}{\rho}\frac{\partial\bar{P}}{\partial\bar{z}} \tag{4}$$

Contributed by the Heat Transfer Division of ASME for publication in the JOURNAL OF HEAT TRANSFER. Manuscript received July 17, 2008; final manuscript received October 22, 2008; published online May 14, 2009. Review conducted by Peter Vadasz.

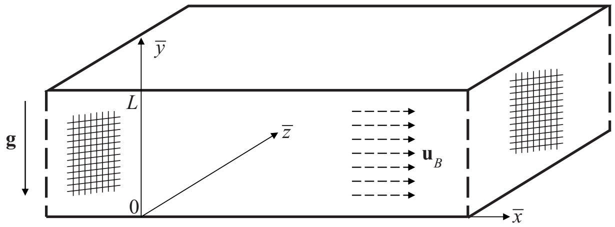

Fig. 1 Sketch of the horizontal porous channel

$$\sigma\frac{\partial\bar{T}}{\partial\bar{t}}+\bar{\mathbf{u}}\cdot\bar{\boldsymbol{\nabla}}\bar{T}=\alpha\bar{\nabla}^2\bar{T}+\frac{\nu}{Kc_p}\left(1+\frac{C_f\sqrt{K}}{\nu}\sqrt{\bar{\mathbf{u}}\cdot\bar{\mathbf{u}}}\right)\bar{\mathbf{u}}\cdot\bar{\mathbf{u}} \tag{5}$$

where σ is the ratio between the average volumetric heat capacity $(\rho c_p)_m$ of the porous medium and the volumetric heat capacity $(\rho c_p)_f$ of the fluid. In Eqs. (1)–(5), the x, y, and z components of velocity are denoted as $\bar{\mathbf{u}}=(\bar{u},\bar{v},\bar{w})$; then the velocity and temperature boundary conditions are expressed as

$$\bar{y}=0:\quad \bar{v}=0=\frac{\partial\bar{T}}{\partial\bar{y}}-\frac{h}{k}(\bar{T}-\bar{T}_w)$$

$$\bar{y}=L:\quad \bar{v}=0=\bar{T}-\bar{T}_w \tag{6}$$

2.1 Nondimensionalization. Let us introduce nondimensional variables such that

$$(\bar{x},\bar{y},\bar{z})=(x,y,z)L,\quad \bar{t}=t\frac{\sigma L^2}{\alpha},\quad (\bar{u},\bar{v},\bar{w})=(u,v,w)\frac{\alpha}{L}$$

$$\bar{T}=\bar{T}_w+T\frac{\nu\alpha}{Kc_p},\quad \bar{p}=p\frac{\mu\alpha}{K} \tag{7}$$

Then, Eqs. (1)–(5) may be rewritten in the form

$$\frac{\partial u}{\partial x}+\frac{\partial v}{\partial y}+\frac{\partial w}{\partial z}=0 \tag{8}$$

$$(1+\eta\sqrt{\mathbf{u}\cdot\mathbf{u}})u=-\frac{\partial p}{\partial x} \tag{9}$$

$$(1+\eta\sqrt{\mathbf{u}\cdot\mathbf{u}})v=-\frac{\partial p}{\partial y}+\mathrm{Ge}T \tag{10}$$

$$(1+\eta\sqrt{\mathbf{u}\cdot\mathbf{u}})w=-\frac{\partial p}{\partial z} \tag{11}$$

$$\frac{\partial T}{\partial t}+u\frac{\partial T}{\partial x}+v\frac{\partial T}{\partial y}+w\frac{\partial T}{\partial z}=\frac{\partial^2 T}{\partial x^2}+\frac{\partial^2 T}{\partial y^2}+\frac{\partial^2 T}{\partial z^2}+(u^2+v^2+w^2)(1+\eta\sqrt{\mathbf{u}\cdot\mathbf{u}}) \tag{12}$$

where $\mathbf{u}=(u,v,w)$ and Ge is the Gebhart number, namely,

$$\mathrm{Ge}=\frac{g\beta L}{c_p} \tag{13}$$

and η is a nondimensional Forchheimer coefficient,

$$\eta=\frac{C_f\sqrt{\mathrm{Da}}}{\mathrm{Pr}}\quad \text{where}\ \mathrm{Da}=\frac{K}{L^2}\ \text{and}\ \mathrm{Pr}=\frac{\nu}{\alpha} \tag{14}$$

The boundary condition (6) may be expressed in dimensionless form,

$$y=0:\quad v=0=\frac{\partial T}{\partial y}-\mathrm{Bi}T$$

$$y=1:\quad v=0=T \tag{15}$$

where Bi is the Biot number, which is defined as

$$\mathrm{Bi}=\frac{hL}{k} \tag{16}$$

2.2 Basic Flow. For the basic solution, we assume a horizontal steady parallel flow in the x-direction and a purely vertical heat flux. Then, the basic state, which has to be analyzed for stability, is given by

$$u_B=\mathrm{Pe}>0,\quad v_B=0,\quad w_B=0$$

$$\frac{\partial p_B}{\partial x}=-\mathrm{Pe}(1+\eta\mathrm{Pe})$$

$$\frac{\partial p_B}{\partial y}=\mathrm{Ge}T_B$$

$$\frac{\partial p_B}{\partial z}=0$$

$$T_B=-\mathrm{Pe}^2(\mathrm{Pe}\,\eta+1)\frac{y^2(\mathrm{Bi}+1)-\mathrm{Bi}y-1}{2(\mathrm{Bi}+1)} \tag{17}$$

where

$$\mathrm{Pe}=\frac{\bar{u}_B L}{\alpha} \tag{18}$$

defines the Péclet number referred to the dimensional uniform base flow velocity $\bar{u}_B$.

2.3 Linearization. Perturbations of the base flow given by Eq. (17) are defined as

$$u=u_B+\varepsilon U,\quad v=v_B+\varepsilon V,\quad w=w_B+\varepsilon W,\quad T=T_B+\varepsilon\theta,$$

$$p=p_B+\varepsilon\mathcal{P} \tag{19}$$

where ε is an asymptotically small perturbation parameter. On substituting Eq. (19) into Eqs. (8)–(12) and neglecting nonlinear terms in the perturbations, i.e., terms of $O(\varepsilon^2)$, one obtains the linearized stability equations, namely,

$$\frac{\partial U}{\partial x}+\frac{\partial V}{\partial y}+\frac{\partial W}{\partial z}=0 \tag{20}$$

$$U(1+2\eta\mathrm{Pe})=-\frac{\partial\mathcal{P}}{\partial x} \tag{21}$$

$$V(1+\eta\mathrm{Pe})=-\frac{\partial\mathcal{P}}{\partial y}+\mathrm{Ge}\theta \tag{22}$$

$$W(1+\eta\mathrm{Pe})=-\frac{\partial\mathcal{P}}{\partial z} \tag{23}$$

$$\frac{\partial\theta}{\partial t}+\mathrm{Pe}\frac{\partial\theta}{\partial x}-\mathrm{Pe}^2(1+\mathrm{Pe}\,\eta)VB(y)=\frac{\partial^2\theta}{\partial x^2}+\frac{\partial^2\theta}{\partial y^2}+\frac{\partial^2\theta}{\partial z^2}+\mathrm{Pe}U(2+3\mathrm{Pe}\,\eta) \tag{24}$$

where B is a function of both Bi and y and is defined as

$$B(y)=y-\frac{\mathrm{Bi}}{2(\mathrm{Bi}+1)} \tag{25}$$

3 Instability With Respect to Rolls

Now, one may differentiate Eqs. (21)–(23) and substitute the results into Eq. (20). Then one may also substitute the velocity components in Eqs. (21) and (22) into Eq. (24) in order to obtain the following pressure/temperature formulation:

$$\left(\frac{1+\mathrm{Pe}\,\eta}{1+2\mathrm{Pe}\,\eta}\right)\frac{\partial^2\mathcal{P}}{\partial x^2}+\frac{\partial^2\mathcal{P}}{\partial y^2}+\frac{\partial^2\mathcal{P}}{\partial z^2}=\mathrm{Ge}\frac{\partial\theta}{\partial y} \tag{26}$$

$$\frac{\partial\theta}{\partial t}+\mathrm{Pe}\frac{\partial\theta}{\partial x}+\mathrm{Pe}^2\left(\frac{\partial\mathcal{P}}{\partial y}-\mathrm{Ge}\,\theta\right)B(y)=\frac{\partial^2\theta}{\partial x^2}+\frac{\partial^2\theta}{\partial y^2}+\frac{\partial^2\theta}{\partial z^2}-\mathrm{Pe}\left(\frac{2+3\mathrm{Pe}\,\eta}{1+2\mathrm{Pe}\,\eta}\right)\frac{\partial\mathcal{P}}{\partial x} \tag{27}$$

Let us assume that the disturbances are given by

$$\mathcal{P}(x,y,z,t)=\Re\{P(y)e^{\lambda t}e^{ia(x\cos\chi+z\sin\chi)}\}$$

$$\theta(x,y,z,t)=\Re\{\Theta(y)e^{\lambda t}e^{ia(x\cos\chi+z\sin\chi)}\} \tag{28}$$

where $\lambda=\lambda_1+i\lambda_2$ is a complex coefficient and χ is the angle between the base flow direction and the propagation direction of the disturbance. The system of Eqs. (26) and (27) now reduces to

$$P''-a^2\left[\left(\frac{1+\mathrm{Pe}\,\eta}{1+2\mathrm{Pe}\,\eta}\right)\cos^2\chi+\sin^2\chi\right]P-\mathrm{Ge}\Theta'=0 \tag{29}$$

$$\Theta''-[\lambda+a^2+ia\mathrm{Pe}\cos\chi-\mathrm{GePe}^2B(y)]\Theta-\mathrm{Pe}^2B(y)P'-ia\mathrm{Pe}\cos\chi\left(\frac{2+3\mathrm{Pe}\,\eta}{1+2\mathrm{Pe}\,\eta}\right)P=0 \tag{30}$$

where primes denote differentiation with respect to y. The boundary condition (15) may be expressed in terms of pressure and temperature as

$$y=0:\quad P'=\mathrm{Ge}\Theta,\quad \Theta'-\mathrm{Bi}\Theta=0;\quad y=1:\quad P'=0=\Theta \tag{31}$$

We will set $\Re(\lambda)=\lambda_1=0$ in order to investigate neutral stability. Moreover, for numerical convenience, we shall also set

$$\gamma=\lambda_2+a\mathrm{Pe}\cos\chi \tag{32}$$

so that Eq. (30) may be rewritten as

$$\Theta''-[a^2+i\gamma-\mathrm{GePe}^2B(y)]\Theta-\mathrm{Pe}^2B(y)P'-ia\mathrm{Pe}\cos\chi\left(\frac{2+3\mathrm{Pe}\,\eta}{1+2\mathrm{Pe}\,\eta}\right)P=0 \tag{33}$$

3.1 Transverse Rolls (χ=0) . The condition $\chi=0$ identifies the transverse roll case. Equations (29), (31), and (33) become

$$P''-a^2\left(\frac{1+\mathrm{Pe}\,\eta}{1+2\mathrm{Pe}\,\eta}\right)P-\mathrm{Ge}\Theta'=0 \tag{34}$$

$$\Theta''-[a^2+i\gamma-\mathrm{GePe}^2B(y)]\Theta-\mathrm{Pe}^2B(y)P'-ia\mathrm{Pe}\left(\frac{2+3\mathrm{Pe}\,\eta}{1+2\mathrm{Pe}\,\eta}\right)P=0 \tag{35}$$

$$y=0:\quad P'=\mathrm{Ge}\Theta,\quad \Theta'-\mathrm{Bi}\Theta=0;\quad y=1:\quad P'=0=\Theta \tag{36}$$

3.2 Longitudinal Rolls ($\chi=\pi/2$) . In the case $\chi=\pi/2$, Eqs. (29), (31), and (33) become

$$P''-a^2P-\mathrm{Ge}\Theta'=0 \tag{37}$$

$$\Theta''-[a^2+i\gamma-\mathrm{GePe}^2B(y)]\Theta-\mathrm{Pe}^2B(y)P'=0 \tag{38}$$

$$y=0:\quad P'=\mathrm{Ge}\Theta,\quad \Theta'-\mathrm{Bi}\Theta=0;\quad y=1:\quad P'=0=\Theta \tag{39}$$

It is important to note the absence of the parameter η in Eqs. (37)–(39). Thus, longitudinal rolls are not affected by the dependence on the Forchheimer term in the momentum equation. Moreover, the problem becomes self-adjoint as one may now set $\gamma=0$ and determine the solution $\{P,\Theta\}$ in terms of real-valued functions.

4 Eigenvalue Problem

Equations (29) and (33) are a pair of coupled homogeneous complex second order ODEs and are subject to the four homogeneous boundary conditions (Eq. (31)). The system always admits a null solution, but it may also be interpreted as an eigenvalue problem for λ where values for λ depend on Ge, Pe, η, χ, and a. Alternatively, incipient instability is given by $\lambda_1=0$; therefore the system may now be regarded as a double eigenvalue problem for Pe and γ, for example, as functions of the remaining parameters. The computation of these eigenvalues requires a further normalization condition to force the solutions for P and Θ to be nonzero; we choose the following:

$$\mathrm{Bi}\Theta'(0)+\Theta(0)=\mathrm{Bi}+1 \tag{40}$$

It also proves convenient to work with the parameter

$$R=\mathrm{GePe}^2 \tag{41}$$

rather than Ge. The critical value of R, which is denoted by R_{cr}, is now determined by seeking the minimum of R as a function of a in the neutral stability curve. In practice this is done by extending the system, Eqs. (29) and (33), by differentiating it with respect to a and by setting $\partial R/\partial a=0$.

4.1 Stability Analysis. In order to solve Eqs. (29), (31), (33), and (40), a numerical solver based on the classical fourth order Runge–Kutta method coupled with the shooting method has been used. In all cases we used 100 intervals, and this, coupled with the fourth order accuracy of the method, yields highly accurate results. The change in R_{cr} as a function of three parameters has been studied. These parameters are the Biot parameter Bi, the angle χ, and the parameter η_+, which is defined as

$$\eta_+=\frac{\eta}{\sqrt{\mathrm{Ge}}} \tag{42}$$

and allows one to remove the explicit dependence on Ge in the physically reasonable range of very small Ge. Indeed, if one substitutes Eq. (42) and the relationship

$$P_+(y)=\frac{P(y)}{\mathrm{Ge}} \tag{43}$$

in Eqs. (29), (31), (33), and (40), one obtains

$$P_+''-a^2\left[\left(\frac{1+\sqrt{R}\,\eta_+}{1+2\sqrt{R}\,\eta_+}\right)\cos^2\chi+\sin^2\chi\right]P_+-\Theta'=0 \tag{44}$$

$$\Theta''-[a^2+i\gamma-RB(y)]\Theta-RB(y)P_+'-ia\sqrt{\mathrm{Ge}R}\cos\chi\left(\frac{2+3\sqrt{R}\,\eta_+}{1+2\sqrt{R}\,\eta_+}\right)P_+=0 \tag{45}$$

$$y=0:\quad P_+'=\Theta,\quad \Theta'-\mathrm{Bi}\Theta=0,\quad \mathrm{Bi}\Theta'+\Theta=\mathrm{Bi}+1;$$
$$y=1:\quad P_+'=0=\Theta \tag{46}$$

It must be mentioned that, on account of Eq. (42), the limit $\eta_+\to 0$ can be interpreted as the limit of the negligible form-drag effect, i.e., the limit of validity of Darcy's law. On the other hand, the limit $\eta_+\to\infty$ is the limit of a very small Gebhart number.

Under the physically realistic assumption of $\mathrm{Ge}\ll 1$, if R is of

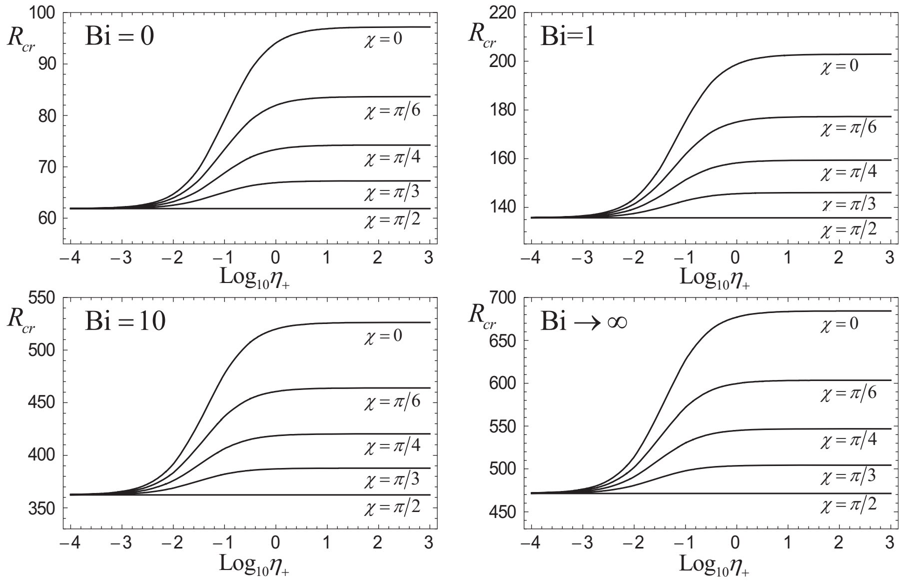

Fig. 2 R_{cr} **as a function of** η_+ **for different values of** χ **for** $\text{Bi}=0,1,10,\infty$

$O(1)$, then the last term on the left hand side of Eq. (45) is of $O(\text{Ge}^{1/2})$. As a consequence, this term is significantly smaller than the other terms. Thus, one can easily infer that neglecting this term allows one to set $\gamma=0$, so that the problem becomes self-adjoint and only admits real solutions for (P,Θ). The Biot number Bi affects the bottom boundary condition. On account of Eq. (25), in the limit of an adiabatic boundary, one has

$$\text{Bi} \to 0 \Rightarrow B(y) = y \tag{47}$$

while, in the limit of a perfectly isothermal boundary, one has

$$\text{Bi} \to \infty \Rightarrow B(y) = y - \frac{1}{2} \tag{48}$$

From Fig. 2 one can see that, for any chosen parameter set, the values of R_{cr} are higher in the case of an isothermal bottom boundary than in the case of an adiabatic bottom boundary. This feature could have been expected. In fact, when examining the basic flow in the case of isothermal bottom boundary ($\text{Bi}\to\infty$), one can see from Eq. (48) that the midplane $y=1/2$ is adiabatic, i.e., $B(1/2)=0$. In other words, in the analysis of the basic flow, the layer with adiabatic bottom boundary is coincident with the upper half of the layer with isothermal bottom boundary, except for the thickness. One sees that R is proportional to L^3. Therefore, one would expect that the critical value of R in the case of a layer with isothermal bottom boundary is eight times that in the case of a layer with adiabatic bottom boundary. The factor of 8 would be exact if in the perturbed flow of the layer with isothermal bottom boundary, the midplane $y=1/2$ is both adiabatic and impermeable. In fact, these conditions are perfectly fulfilled by the basic flow but not by the disturbances. It should be mentioned, however, that the lower half of the layer with isothermal bottom boundary is expected to be affected only marginally by roll disturbances as the midplane $y=1/2$ is, in the basic state, hotter than the bottom boundary $y=0$.

In Fig. 2 one may also notice that R_{cr}, for every Biot number Bi, is not affected by the orientation angle χ in the limit of validity of Darcy's law, $\eta_+\to 0$. On the contrary, in the limit of important form-drag effects with $\text{Ge}\ll 1$ ($\eta_+\to\infty$), one finds an important dependence of R_{cr} on the orientation of the oblique rolls. In particular, longitudinal rolls ($\chi=\pi/2$) appear to be the most unstable. For longitudinal rolls, R_{cr} is independent of η_+. This feature is evident from Eqs. (44)–(46) as the parameter η_+ disappears from the equations when $\chi=\pi/2$. For $\eta_+\to 0$ there appears an asymptotic behavior described in Table 1. For $\eta_+\to\infty$, a different asymptotic value of either R_{cr} or a_{cr} is reached for every χ. The highest asymptotic values of R_{cr} or a_{cr} refer to transverse rolls ($\chi=0$). These values are reported in Table 1.

Figure 3 shows the plots of the critical wavenumber a_{cr} versus η_+ for different orientation angles χ and Biot numbers Bi. The qualitative behavior of a_{cr} is similar to that of R_{cr}. The curves display the asymptotic behavior for $\eta_+\to 0$ as for $\eta_+\to\infty$. Both the lower and the upper asymptotic values are specified in Table 1.

The plots reported in Figs. 4–7 suggest a not too strong dependence of $\Theta_{\text{cr}}(y)$ on both η_+ and χ. In particular, for $\eta_+=10^{-5}$, the solid and dashed lines corresponding, respectively, to $\chi=0$ and $\chi=\pi/4$ are perfectly coincident. Indeed, the eigenvalue problem (44)–(46) becomes independent of χ in the limit $\eta_+\to 0$ (i.e., in the limit of validity of Darcy's law). The temperature profiles $\Theta_{\text{cr}}(y)$ represented in Fig. 4 refer to an adiabatic bottom boundary, while those reported in Figs. 5–7 refer to an imperfectly isothermal boundary ($\text{Bi}=1,10$) and to a perfectly isothermal boundary ($\text{Bi}\to\infty$). Due to Eq. (46), all the profiles reported in Figs. 4–7 display at $y=0$ a fixed temperature, $\Theta(0)=(\text{Bi}+1)/(\text{Bi}^2+1)$, and a fixed heat flux, $\Theta'(0)=\text{Bi}(\text{Bi}+1)/(\text{Bi}^2+1)$.

Figures 8–11 refer to critical conditions and show the isotherms, $\theta=$const, and the streamlines of the two-dimensional velocity disturbance field (U,V), respectively, for the orientation angle $\chi=0$ and $\eta_+=10^3$. In fact, from Eq. (23), one has $W=0$ as Eq. (28) predicts for $\chi=0$ that $\mathcal{P}$ is independent of z. For the adiabatic case, $\text{Bi}=0$ (Figs. 8 and 9), one may see that the velocity rolls are spread over the whole channel width and are almost symmetric with respect to the horizontal midplane. When the bottom boundary is isothermal, $\text{Bi}\to\infty$ (Figs. 10 and 11), the velocity rolls are placed predominantly within the upper part of the chan-

Table 1 **Asymptotic values of** a_{cr} **and** R_{cr} **for different Biot numbers**

	$\eta_+\to 0$		$\eta_+\to\infty$; $\chi=0$	
Bi	a_{cr}	R_{cr}	a_{cr}	R_{cr}
0	2.4483	61.867	3.0342	97.184
1	2.9697	135.71	3.6482	202.88
10	4.2573	362.32	5.0722	526.30
∞	4.6752	471.38	5.5616	684.36

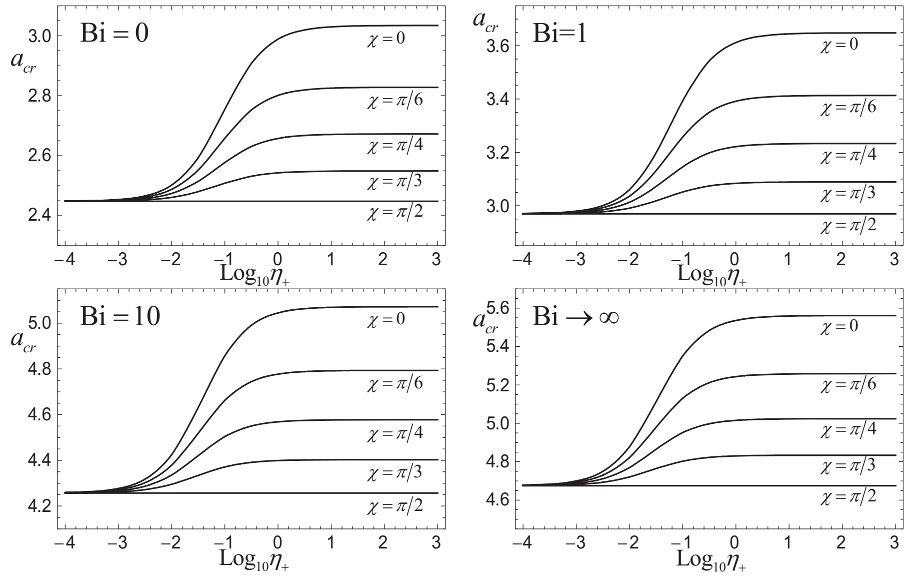

Fig. 3 a_{cr} **as a function of** η_+ **for different values of** χ **for Bi=0,1,10,∞**

nel. This upward displacement is justified since the fluid is unstably stratified only in the upper part of the porous layer. In fact, in the basic flow solution Eq. (17) for Bi→∞, the horizontal midplane is hotter than the boundary planes.

5 Conclusion

A stability analysis of the basic parallel uniform flow in a horizontal porous layer with impermeable boundaries has been per-

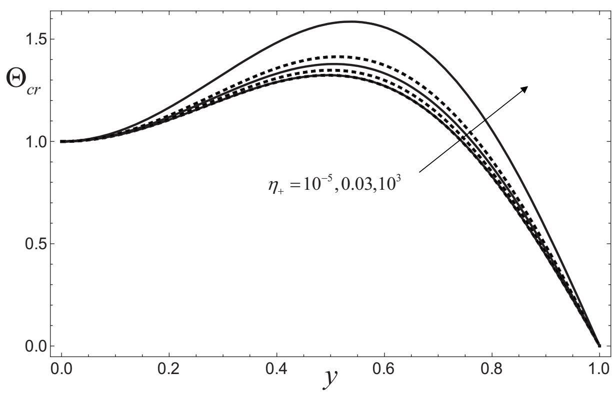

Fig. 4 Plots of Θ_{cr} **as a function of** y **for Bi=0 and** $\eta_+ = 10^{-5}, 0.03, 10^3$**. Solid lines refer to** $\chi=0$**, while dashed lines refer to** $\chi=\pi/4$**.**

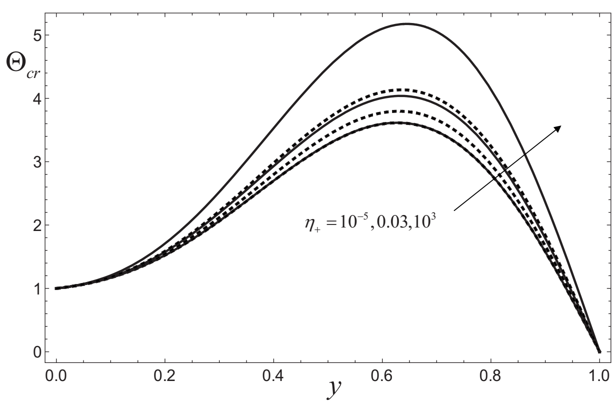

Fig. 5 Plots of Θ_{cr} **as a function of** y **for Bi=1 and** $\eta_+ = 10^{-5}, 0.03, 10^3$**. Solid lines refer to** $\chi=0$**, while dashed lines refer to** $\chi=\pi/4$**.**

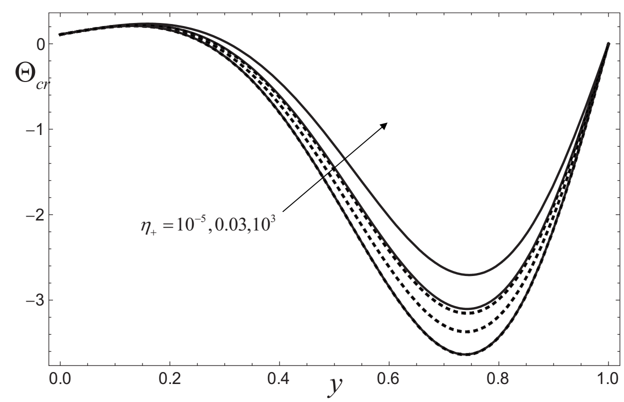

Fig. 6 Plots of Θ_{cr} **as a function of** y **for Bi=10 and** $\eta_+ = 10^{-5}, 0.03, 10^3$**. Solid lines refer to** $\chi=0$**, while dashed lines refer to** $\chi=\pi/4$**.**

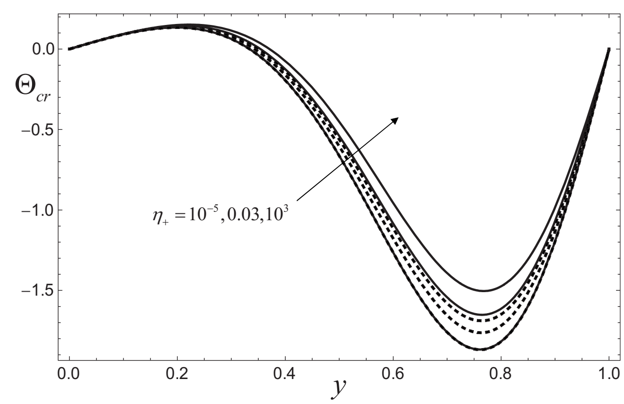

Fig. 7 Plots of Θ_{cr} **as a function of** y **for Bi→∞ and** $\eta_+ = 10^{-5}, 0.03, 10^3$**. Solid lines refer to** $\chi=0$**, while dashed lines refer to** $\chi=\pi/4$**.**

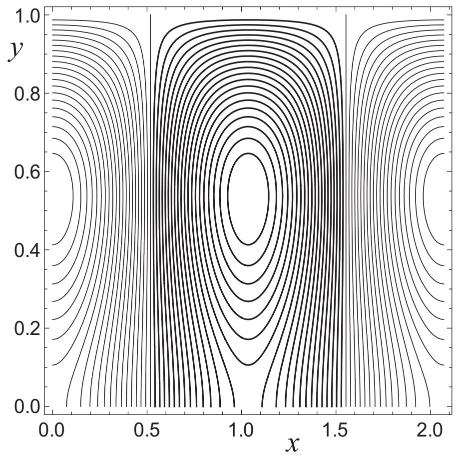

Fig. 8 Disturbance isotherms for Bi=0, $\eta_+=10^3$, and $\chi=0$

formed. The Darcy–Forchheimer model, together with the Oberbeck–Boussinesq approximation, has been adopted. The basic temperature profile is nonlinear due to the effect of viscous dissipation. The top boundary plane has been taken to be isothermal. The bottom boundary has been assumed to be subject to a third kind boundary condition described in the dimensionless equations through the Biot number, Bi. The conditions of vanishing heat flux and of uniform temperature at the bottom boundary

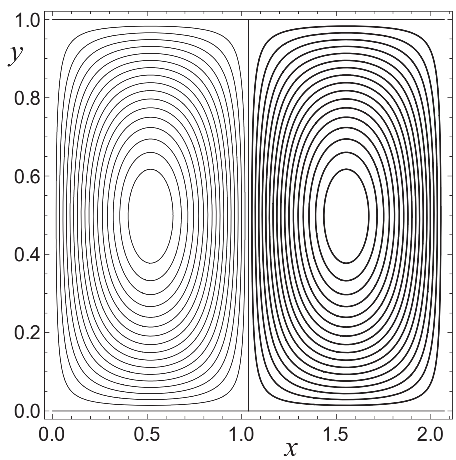

Fig. 9 Streamlines for Bi=0, $\eta_+=10^3$, and $\chi=0$

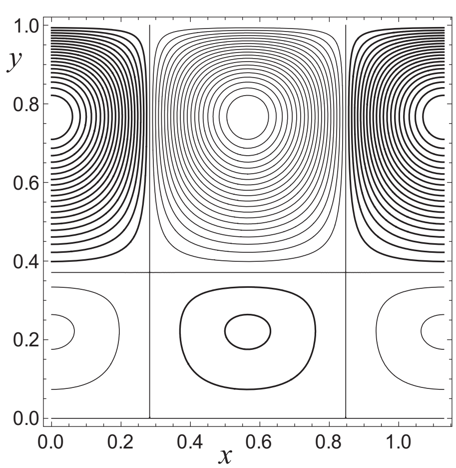

Fig. 10 Disturbance isotherms for Bi→∞, $\eta_+=10^3$, and $\chi=0$

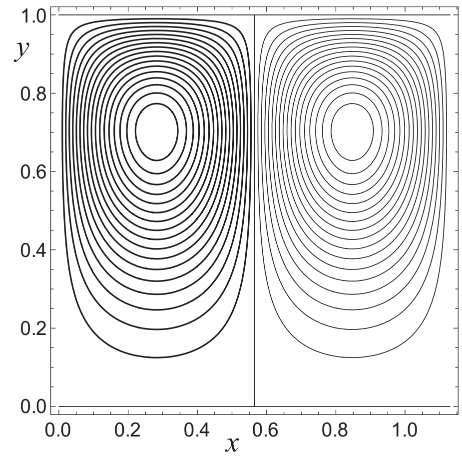

Fig. 11 Streamlines for Bi→∞, $\eta_+=10^3$, and $\chi=0$

are mathematically expressed as two limiting cases $\mathrm{Bi}\to 0$ (adiabatic boundary) $\mathrm{Bi}\to\infty$ (isothermal boundary). Arbitrarily orientated roll disturbances have been studied by adopting a pressure-temperature formulation. The resulting eigenvalue ODE problem has been solved numerically by means of a fourth order Runge–Kutta method coupled with the shooting method.

The main results obtained are the following:

1. The governing parameter describing the onset of convective instabilities is $R=\mathrm{GePe}^2$, where Ge is the Gebhart number and Pe is the Péclet number.
2. Under the physically reasonable assumption $\mathrm{Ge}\ll 1$, the eigenvalue ODE problem becomes self-adjoint, thus admitting real solutions.
3. The most unstable rolls are the longitudinal ones.
4. The critical wavenumber and the critical value of R for the onset of longitudinal rolls are independent of the form-drag coefficient.
5. The critical wavenumber and the critical value of R for the onset of transverse or oblique rolls other than longitudinal ones depend on the form-drag coefficient.
6. The layer with an isothermal bottom boundary is more stable than the layer with an adiabatic bottom boundary.

Nomenclature

a = nondimensional wavenumber, Eq. (28)
Bi = Biot number, Eq. (16)
$B(y)$ = nondimensional function, Eq. (25)
c_p = specific heat at constant pressure
C_f = Forchheimer parameter
Da = Darcy number, Eq. (14)
g = modulus of gravitational acceleration
$\mathbf{g}$ = gravitational acceleration
Ge = Gebhart number, Eq. (13)
h = external heat transfer coefficient
K = permeability
k = effective thermal conductivity
L = channel height
n = integer number
p = nondimensional pressure, Eq. (7)
$\mathcal{P}$ = nondimensional pressure disturbance, Eq. (19)
$P(y)$ = nondimensional function, Eq. (28)
$P_+(y)$ = nondimensional function, Eq. (43)
Pe = Péclet number, Eq. (18)
Pr = Prandtl number, Eq. (14)
R = nondimensional parameter, Eq. (41)
$\Re$ = real part
t = nondimensional time, Eq. (7)

T = nondimensional temperature, Eq. (7)
$\bar{T}_w$ = boundary temperature or external temperature
u, v, w = nondimensional velocity components, Eq. (7)
U, V, W = nondimensional velocity disturbances, Eq. (19)
x, y, z = nondimensional coordinates, Eq. (7)

Greek Symbols

α = effective thermal diffusivity
β = volumetric coefficient of thermal expansion
γ = reduced exponential coefficient, Eq. (32)
η = nondimensional Forchheimer parameter, Eq. (14)
η_+ = nondimensional modified Forchheimer parameter, Eq. (42)
ε = perturbation parameter, Eq. (19)
θ = nondimensional temperature disturbance, Eq. (19)
$\Theta(y)$ = nondimensional function, Eq. (28)
λ = exponential coefficient, Eq. (28)
λ_1, λ_2 = real and imaginary parts of λ
ν = kinematic viscosity
ρ = mass density
σ = heat capacity ratio
χ = angle between the propagation direction of the disturbance and the x-axis

Superscript and Subscripts

$-$ = dimensional quantity
B = base flow
cr = critical value

References

[1] Horton, C. W., and Rogers, F. T., Jr., 1945, "Convection Currents in a Porous Medium," J. Appl. Phys., **16**, pp. 367–370.
[2] Lapwood, E. R., 1948, "Convection of a Fluid in a Porous Medium," Proc. Cambridge Philos. Soc., **44**, pp. 508–521.
[3] Nield, D. A., and Bejan, A., 2006, *Convection in Porous Media*, 3rd ed., Springer, New York.
[4] Rees, D. A. S., 2000, "Stability of Darcy-Bénard Convection," *Handbook of Porous Media*, K. Vafai, ed., Dekker, New York, pp. 521–558.
[5] Tyvand, P. A., 2002, "Onset of Rayleigh-Bénard Convection in Porous Bodies," *Transport Phenomena in Porous Media II*, D. B. Ingham and I. Pop, eds., Elsevier, New York, pp. 82–112.
[6] Prats, M., 1966, "The Effect of Horizontal Fluid Flow on Thermally Induced Convection Currents in Porous Mediums," J. Geophys. Res., **71**, pp. 4835–4838.
[7] Rees, D. A. S., Magyari, E., and Keller, B., 2005, "Vortex Instability of the Asymptotic Dissipation Profile in a Porous Medium," Transp. Porous Media, **61**, pp. 1–14.
[8] Barletta, A., Celli, M., and Rees, D. A. S., 2009, "The Onset of Convection in a Porous Layer Induced by Viscous Dissipation: A Linear Stability Analysis," Int. J. Heat Mass Transfer, **52**, pp. 337–344.
[9] Storesletten, L., and Barletta, A., 2009, "Linear Instability of Mixed Convection of Cold Water in a Porous Layer Induced by Viscous Dissipation," Int. J. Therm. Sci., **48**, pp. 655–664.